Chapter 5
Metal Surface Engineering Based on Formation of Nanoscaled Phase Protective Layers

V. M. Ledovskykh, Yu. P. Vyshnevska, I. V. Brazhnyk, and S. V. Levchenko

5.1 Introduction

Surface engineering for obtaining nanoscale protective and functional coatings with enhanced properties constitutes a multidiscipline challenge and requires combination of fundamental knowledge from different areas, including electrochemistry, physics of condensed matter, and chemistry of nanoscaled systems. One of the approaches for implementing such surface modification is the purposeful engineering of the specific conditions and utilization of spontaneous processes including the process of metal ionization in a controlled manner to achieve the formation of coatings with desired structure, thickness, morphology, and alignment.

Over a past decade, the theoretical models that represent the mechanism of action of the inhibitive additives on the dissolution and degradation processes of the metal surface in different media have been significantly improved. For the additives that are capable of forming slightly soluble compounds with the metal ions, the modern models predict the formation of thin phase layers on the metal surface. Such layers may serve as protective, functional, or multifunctional coatings, while their composition, structure, and morphology may be adjusted in a wide range by tuning the additive concentrations and engineering favorable conditions and deposition

V. M. Ledovskykh · S. V. Levchenko
National Aviation University, Kyiv, Ukraine

Yu. P. Vyshnevska (✉)
National Technical University of Ukraine "Igor Sikorsky Kyiv Polytechnic Institute", Kyiv, Ukraine

Institute for Renewable Energy NAS of Ukraine, Kyiv, Ukraine

I. V. Brazhnyk
Gimasi SA Ukraine R&D Centre, Via Luigi Lavizzari, Mendrisio, Switzerland

O. Fesenko, L. Yatsenko (eds.), *Nanocomposites, Nanostructures, and Their Applications*, Springer Proceedings in Physics 221,
https://doi.org/10.1007/978-3-030-17759-1_5

regime. Of particular interest are the binary inhibitive mixtures that include additives of different nature and mechanism of action that demonstrate extremely protective efficiency. At the same time, the complete theoretical representation for combined action of the individual inhibitive and modification mixture components on the formation of phase protective layers in such multicomponent systems to date has not been proposed.

In this work, the influence of concurrent and complement effects within inhibitive mixtures on the thickness, structural parameters, and barrier properties of the obtained coatings has been investigated.

5.2 Materials and Experimental Methods

Individual inhibitors and their binary compositions based on XO_n^- anions, and based on anions, that may form the slightly soluble salts with Fe^{2+} cations (SiO_3^{2-} and polyhexametylene guanidine (PHMG)), for inhibiting the carbon steel corrosion in neutral media, are investigated. Aqueous saline solutions have the following composition: 0.3 g/l NaCl, 0.3 g/l Na_2SO_4, and 0.3 g/l $NaHCO_3$.

Determination of the inhibitor efficiency was performed gravimetrically according to the standard procedure. Exposure time at 25 °C temperature of carbon steel 08kp in neutral solutions was 168 h. The ratio of the solution volume (ml) to the area of metal sample (cm^2) was 10:1. The inhibition efficiency was determined by the equation $Z = \left[\left(K_m - K_m^{'}\right)/K_m\right] \cdot 100\%$ and the inhibition coefficient by the equation $\gamma = K_m/K_m^{'}$, where K_m, $K_m^{'}-$ is the corrosion rate of metal in solutions without and with inhibitor ($K_m = \Delta m/(S \cdot \tau)$, where Δm is the loss of the sample weight, g; S is the sample area, m^2; and τ is the exposure time, h).

Polarization measurements were carried out in the potentiostatic regime in a three-electrode cell with separated cathodic and anodic compartments. Carbon steel 08kp was used as the working electrode, platinum as the counter-electrode, and an Ag|AgCl|KCl (sat.) electrode as the reference one. In this paper, the potential values are given with respect to the normal hydrogen electrode potential.

Investigation of the morphological characteristics and elemental composition of the surface protective films of the inhibitive compositions and distribution of elements into the phase film were carried out with the scanning electron microscope (EVO-50, Zeiss, Germany) equipped with the energy-dispersive detector (INCA PENTA FET × 3, Oxford Instruments, Co., UK) and using Auger microprobe JAMP-9500F in the scanning electron microscopy mode. The energy of the electron beam was 3 keV and the current was 0.5 μA. During the profiling, the surface of the samples was bombarded with argon ions (ion etching) with an energy of 4 keV. The pickling rate is 40 Å/min.

5.3 Results and Discussion

Formation of phase layers on a metal surface is extensively used for metal protection. In particular, such mechanism is utilized by the passivation-type inhibitors for protection of steel in aqueous saline solutions where the dissolved molecular oxygen is found to be the main corrosive agent. Due to a possibility of direct and lateral depolarizer transport toward the metal surface, the inhibition of the cathodic reduction reaction may be complicated to be achieved in practice. For this reason, passivators mainly target the anodic reaction of metal ionization via formation of phase protective films on the metal surface.

In most cases, the mechanism implies the formation of the protective oxide layers (oxide passivation) or deposition of slightly soluble salts in a form of a dense film that blocks the metal surface (salt passivation). The first group includes oxyanions XO_n^- (nitrites, clorates, chromates, and others), while the second group may be illustrated with silicates, phosphates, as well as guanidine derivatives that may form slightly soluble complex salts with iron cations [1–6].

Protective efficiency may be further improved via development of inhibitive mixtures that utilize synergistic effects within its individual components wherein the optimal concentration ratio virtually complete protection can be achieved [7–10]. Extremely high protective efficiency combined with the ability to control the composition of the formed phase layers by optimizing the mixture components and concentration ratio predetermines the expediency of in-depth research for building theoretical representation of the processes and regularities of synergistic phenomena in such multicomponent systems.

The thermodynamic approach for analysis of redox transformations of the reagents and products is the key for understanding the reaction mechanism in studied multicomponent systems. The Pourbaix diagram [11] for the Fe-H_20 system (Fig. 5.1) provides an ability to determine the conditions for the formation of oxide films on the metal surface depending on the electrode potential of possible equilibria and pH value of the medium.

The pH value of the blank solution greatly affects the state of the system and in particular the metal surface. In the case of a shift above pH 9 and crossing the *line 7* of the diagram, the system is being transferred from the hydrated Fe (II) ions toward the hydrated iron (II) hydroxide according to the following reaction:

$$Fe^{2+} + 2H_2O = Fe(OH)_2 + 2H^+$$

SEM images confirm the significant morphology changes caused by the oxide films formed under different pH conditions in blank solution (Figs. 5.2 and 5.3). Thus, pH 9 constitutes the hydrogen value of hydrate formation for iron (II) that is a thermodynamically stable form under these conditions. This is found to be in a good agreement with elemental composition of the surface layer that contains a significant amount of oxygen and delivers very slight reduction in the corrosion rate owing to deceleration of the anodic reaction of metal ionization. This is also in line

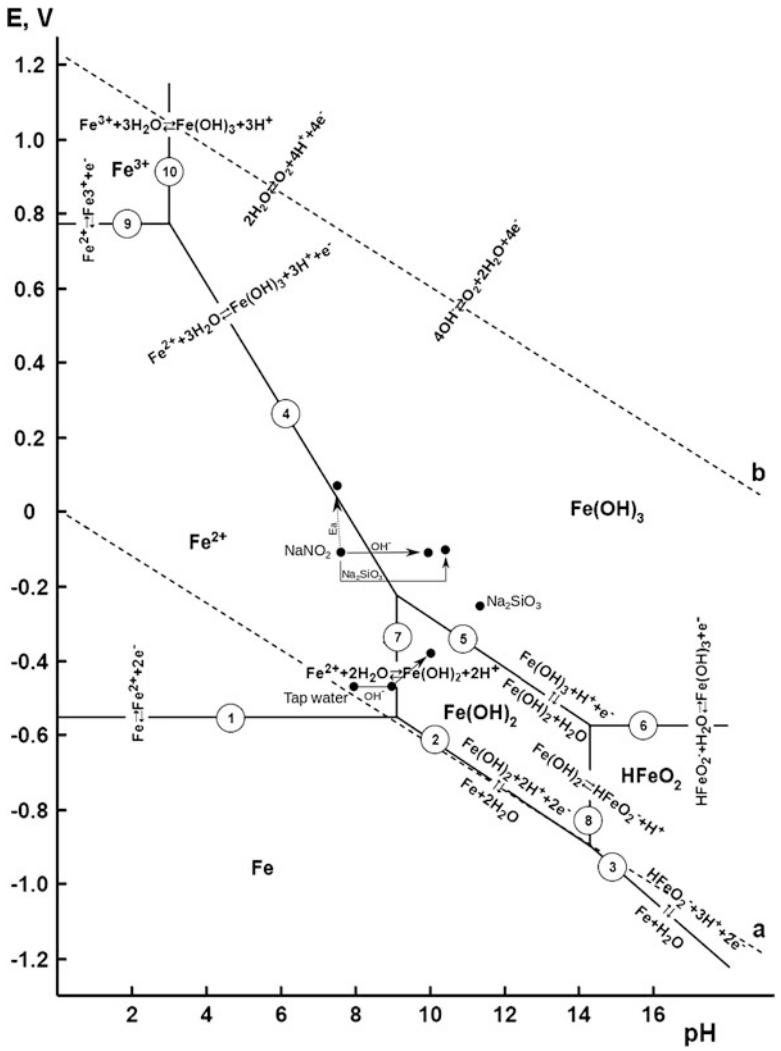

Fig. 5.1 Pourbaix diagram of the Fe-H_2O system

with Evans and Rozenfeld representation that casted a doubt on the possibility of achieving the efficient passivation of steel using deposited iron (II) hydroxides [1].

Oxyanions with oxidative action like NO_2^- have the active electron pair on the sp^2−hybridized orbital on the central nitrogen atom that results in its adsorption properties on the metal surface.

This representation is supported by the fact that the nitrate ion, despite being coordinated analogue virtually, does not affect the corrosion process due to lack of such electron pairs [6].

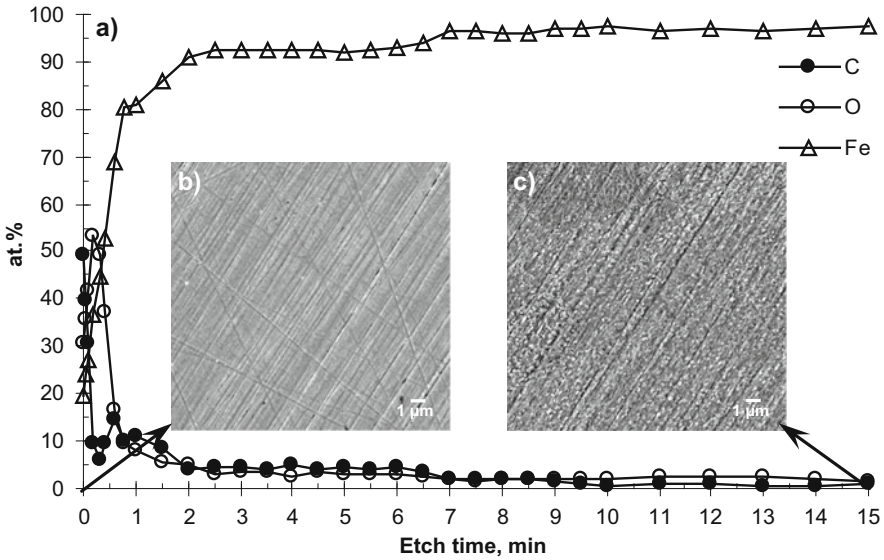

Fig. 5.2 Elemental composition of the surface of an unexposed sample obtained using Auger spectroscopy with ion etching against etching time (**a**) and surface morphology before (**b**) and after etching (**c**)

Infusion of NO_2^- to neutral aqueous saline solution leads to a shift of the steel corrosion potential toward a positive direction from $E_{corr} \cong -0.42$ V to -0.1 V and decrease in the corrosion rate due to inhibition of anodic reaction (Fig. 5.4). At the same time, the additive virtually does not affect the kinetics of the cathodic reaction while the anodic process of metal ionization remains in active area (Figs. 5.1 and 5.4).

Under these conditions, the morphology studies show generally a uniform film structure with marked signs of local corrosion damage (Fig. 5.5), while the ion etching of the surface show the presence of a nanoscale protective layer with typical thickness of 15–20 nm (Fig. 5.6).

The presence of nitrite ions has been confirmed using Auger spectroscopy that showed presence of 4% of nitrogen within a surface layer of the sample (Fig. 5.6). The surface profiling using ion etching showed sharp decrease in nitrogen concentration falling to zero levels after 1 min of etching that is also in line with theoretical expectations (Fig. 5.6).

It should also be noted that the morphology of the support plate under a protective layer is greatly affected by the film formation process during exposition (Fig. 5.6b). Figure 5.3c shows a typical phase domain structure after removing the surface layer using ion etching. In contrast, the morphology of the support plate after etching of the film formed in the presence of $NaNO_2$ shows a marked relief structure with a partially nonlinear pattern that does not match typical signs of mechanical treatment. Such results also could not be explained by the assumption that the

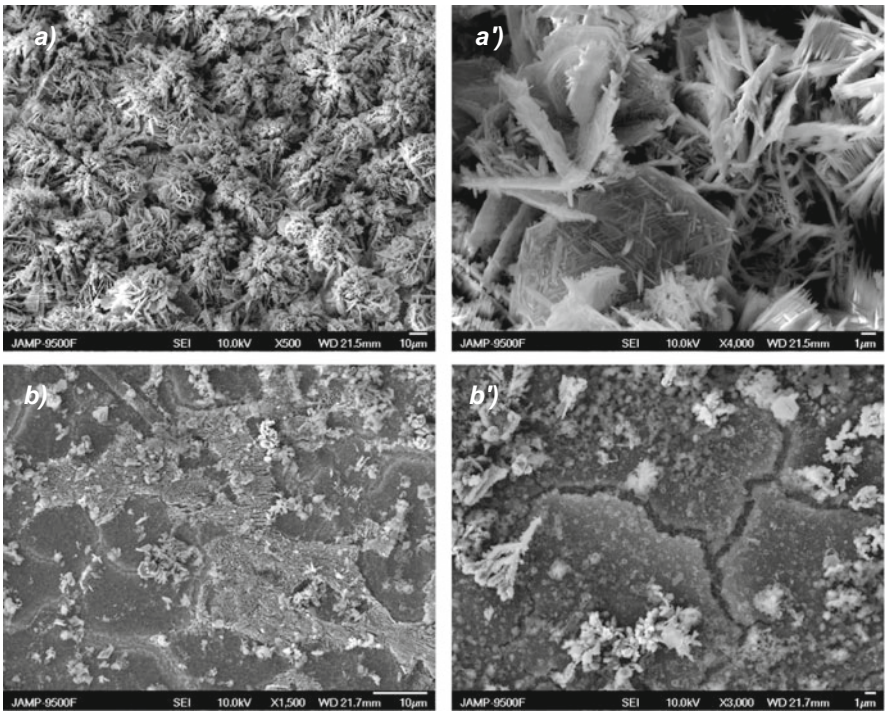

Fig. 5.3 Sample morphology: (***a, a′***) after 168 h exposition in blank solution at pH 7.3, (***b, b′***) after 168 h exposition in blank solution at pH 10

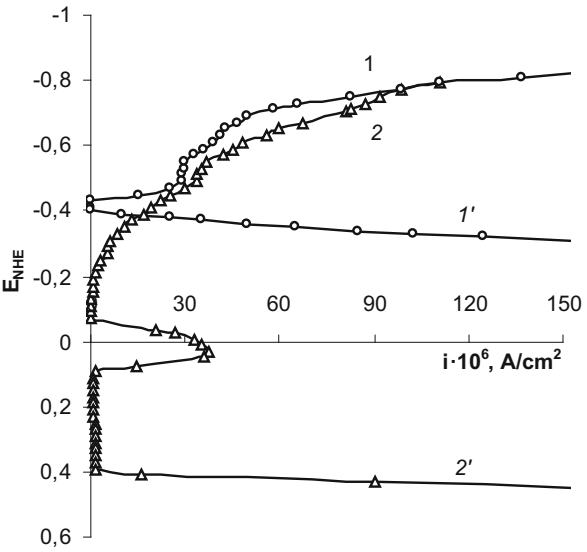

Fig. 5.4 Cathodic (1, 2) and anodic (*1′*, *2′*) polarization curves for carbon steel in *1, 1′*, background aqueous saline solution; *2*, *2′*, in the presence of $NaNO_2$ (30 mmol/l) at pH 7.38

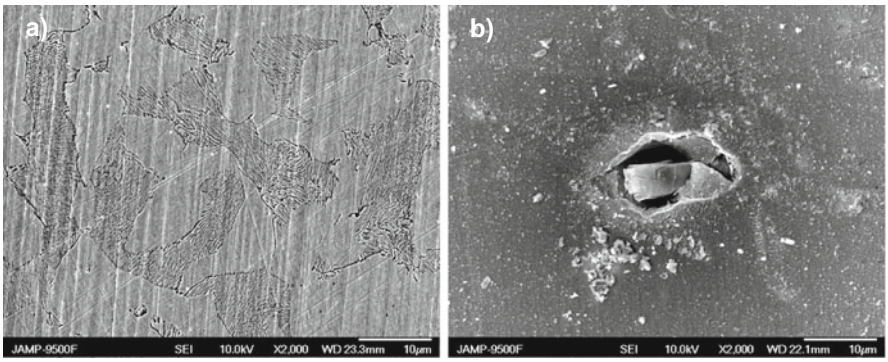

Fig. 5.5 Morphology of the protective film after 18 h (**a**) and 168 h (**b**) of exposition in the presence of $NaNO_2$ (30 mmol/l) at pH 7.38

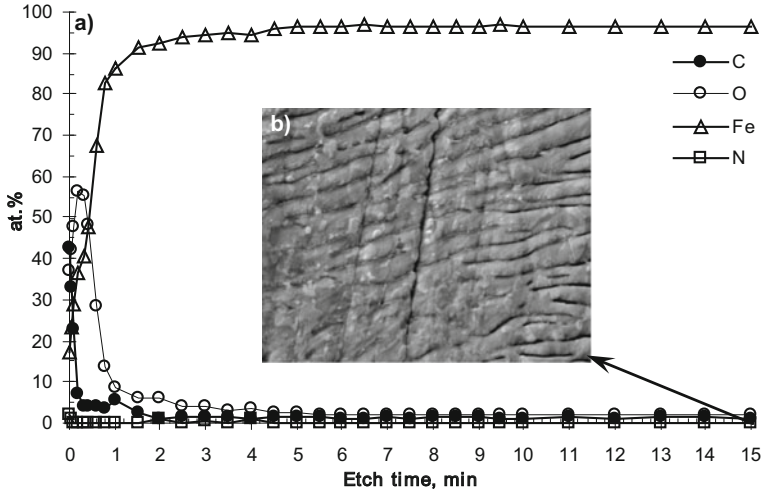

Fig. 5.6 Elemental composition of the protective film formed in the presence of $NaNO_2$ (30 mmol/l) obtained using Auger spectroscopy with ion etching against etching time (**a**) and surface morphology after etching (**b**)

protective film has been etched only partially as the elemental composition stabilizes as expected for plain steel values after 5 min of ion etching. Based on the obtained results, we may conclude that the presence of NO_2^- ions may affect the metal ionization process on such an extent that it could lead to a macroscopic change in the morphology of the metal surface.

Analysis of the polarization measurements shows the electrode potential must be shifted to 1.0 V for transferring the metal surface to a passive state. According to the Pourbaix diagram, such shift corresponds to a transition toward a state of thermodynamically stable hydrated ions of iron (III) (Fig. 5.1) that are capable of forming protective phase layers on the metal surface.

The pH value of the medium also affects the protective efficiency and mechanism of action of the NO_2^- ion. Near the *line 4* of the Pourbaix diagram, inhibitive efficiency of the nitrite ion rises significantly that may be attributed to a phenomenon when under this condition the reduction of the inhibitor with assimilation of the electron that is released during oxidizing of iron (II) to iron (III) ions. Shifting the Fe-H_2O system toward a state with thermodynamically stable hydrated iron (III) oxides leads to a formation of dense phase layers on the metal surface according to the reaction:

$$Fe^{2+} + 3H_2O = Fe(OH)_3 + 3H^+ + \overline{e}$$

Higher inhibitive efficiency at a higher pH value is also in line with the SEM images that reveal a much smoother morphology of the protective film, while the analysis of its elemental composition shows significant decrease in the nitrogen content that is on one order of magnitude lower than at pH 7.38 (Fig. 5.7).

Investigation of the kinetics of the electrode processes in the presence of $NaNO_2$ under pH 10 using the polarization measurements shows notable increase in the cathodic reaction rate, while the anodic one is significantly decelerated owing to a passivation of the metal surface with protective oxide film (Fig. 5.8).

In contrast to oxyanions, the inhibitive properties of silicates, phosphates, and carbonates of alkaline metals are due to their ability to form slightly soluble salts with iron cations with subsequent formation of dense phase protective layers on the metal surface. At the same time, analysis of the protective mechanism of such compounds should take into account their ability to undergo hydrolysis in aqueous solutions by the anion of weak acid that will lead to a significant alkalization of the medium. For this reason, the protective performance of such additives should be assessed in conjunction with the sole alkalinization effect without inhibitor that will ensure comparable conditions and reliability of the results.

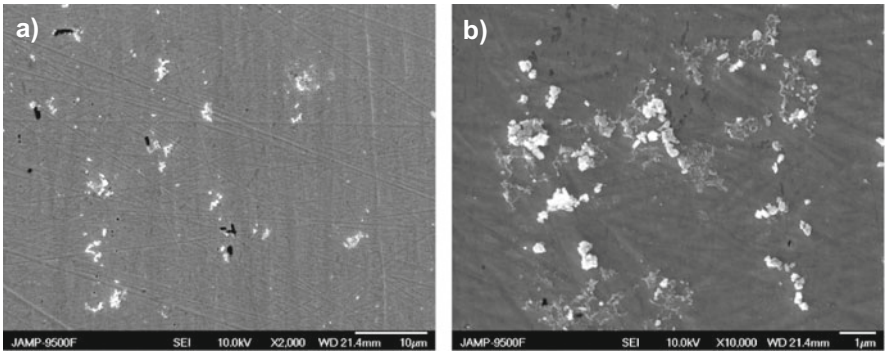

Fig. 5.7 SEM images of the sample after immersion into solution with $NaNO_2$ (30 mmol/l) at pH 10

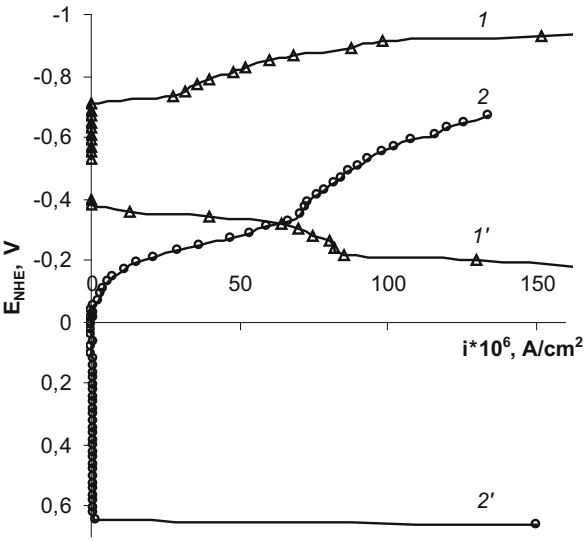

Fig. 5.8 Cathodic (*1, 2*) and anodic (*1′, 2′*) polarization curves for carbon steel in *1, 1′*, background aqueous saline solution; *2, 2′*, in the presence of $NaNO_2$ (30 mmol/l) at pH 10

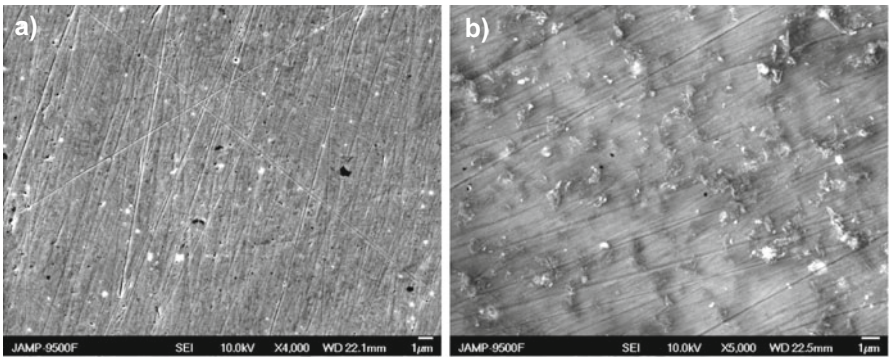

Fig. 5.9 Morphology of the protective film after 18 h (**a**) and 168 h (**b**) exposition in solution with Na_2SiO_3 (30 mmol/l) at pH 11.2

Increase in pH value and shift of the corrosion potential of steel result in the formation of nanoscaled uniform protective layers on the metal surface (Figs. 5.9 and 5.10). It should be noted that after 168 h of exposition (Fig. 5.9b), marks of mechanical treatment may still be observed.

Thus, in contrast to nitrite, Na_2SiO_3 does not tend to provoke metal ionization and is capable of better preserving the original structure of the metal surface under the protective film that is in line with theoretical expectation based on the difference in the mechanism of action.

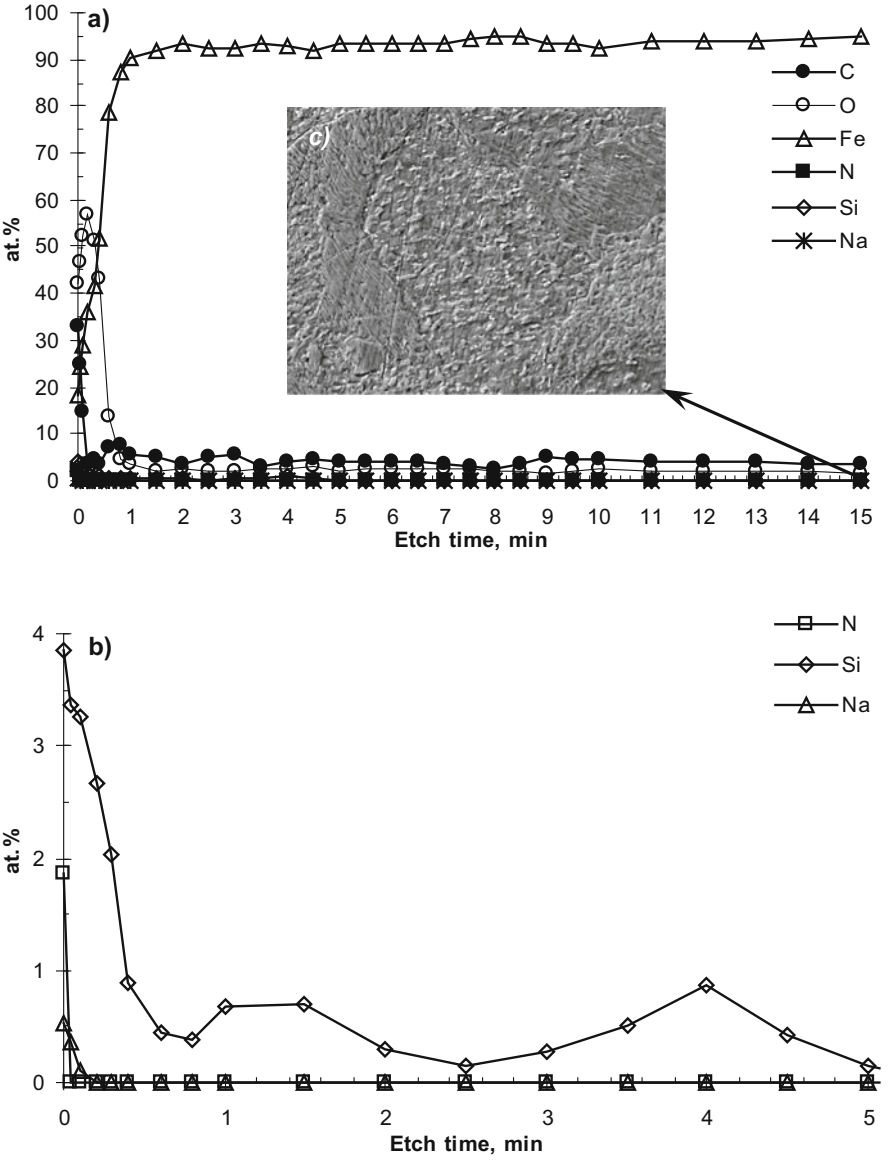

Fig. 5.10 Elemental composition of the protective film formed in the presence of Na_2SiO_3 (30 mmol/l) at pH 11.2 obtained using Auger spectroscopy with ion etching against etching time (**a**), nitrogen, silicon, and sodium atom distribution within the surface layer (**b**), and sample morphology after ion etching (**c**)

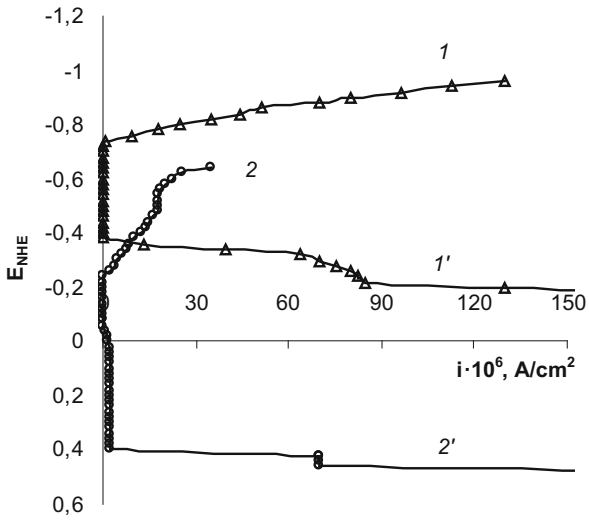

Fig. 5.11 Cathodic (*1*, *2*) and anodic (*1′*, *2′*) polarization curves for carbon steel: *1*, *1′*, background aqueous saline solution at pH 10; *2*, *2′*, in the presence of Na_2SiO_3 (30 mmol/l)

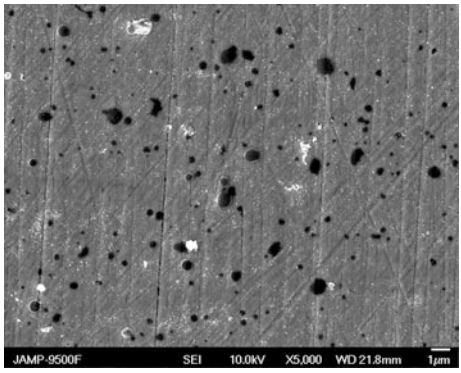

Fig. 5.12 Morphology of the protective film formed in the presence of PHMG (30 mmol/l)

Auger spectra analysis with ion etching revealed the elemental composition and its distribution within the protective layer. The film thickness is found to be ~40 nm with significantly increased content of silicon and oxygen (Fig. 5.10).

According to the polarization measurements, the presence of silicate additive leads to passivation of the metal surface and emergence of the complete passivation zone in the anodic portion of polarization curve (Fig. 5.11).

Similar results may be obtained with organic ligands that are capable of forming slightly soluble complex salts with the metal cations, in particular with polyhexamethylene guanidine (PHMG). Formation of the phase layer of Fe-PHMG complexes (Fig. 5.12) delivers slight metal protection, while its efficiency is significantly lower than in acidic medium [7].

Auger analysis confirms the formation of a phase layer with significant content of carbon and nitrogen of 49.3 and 20.6 at.%, respectively, while the iron content is 12.2 at.% that is found to be in good agreement with theoretical expectations.

It should be noted that despite uniform morphology without signs of local corrosion damage, the protective efficiency of sole PHMG under these conditions falls below other studied inorganic additives reaching typical values of 40%. Such efficiency may be attributed to the fact that PHMG as a complexing type inhibitor requires sufficient amount of iron cations in order to form a dense phase layer. Thus, we may predict that in the case of successful engineering of favorable conditions for complexation process, the PHMG protective efficiency may be significantly improved.

One of the approaches for achieving higher efficiency as well as better control over the protective layer composition, microstructure, and morphology is the development of theoretical representation of the combined action of the additives in multicomponent systems.

It was found, that binary mixtures that combine inhibitive additives with different mechanisms of action may exhibit synergistic effects and deliver improved protective performance. The dependence of protective efficiency against concentration ratio of their components in such cases is found to be extreme where in maxima the most significant protective effect may be achieved [12].

The mechanism of action of synergistic inhibitive compositions is largely determined by their individual characteristics: the additives of oxidative oxoanions contribute to the formation of nanoscaled oxide films on the metal surface, while the inhibitors of salt passivation may alkalize the medium and modify the films with the slightly soluble salts with the iron cations, which eliminates the negative factor of pitting formation as a result of the local damage of the passive layers.

In particular, the synergistic mixtures of $NaNO_2 + Na_2SiO_3$ ensure the formation of a uniform protective layer without signs of local damage that is typical for sole $NaNO_2$ (Fig. 5.13).

The elemental composition of the surface phase layers formed in the presence of synergistic mixtures of $NaNO_2 + Na_2SiO_3$ at pH 10.2 showed a decrease in

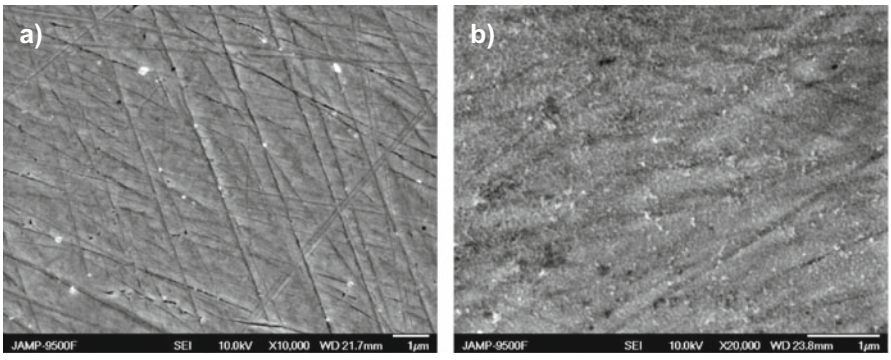

Fig. 5.13 Morphology of the surface layers formed in the presence of synergistic inhibitive mixture of $NaNO_2$ (10 mmol/l) + Na_2SiO_3 (20 mmol/l) at pH 10. Exposure time: (**a**) of 18 h and (**b**) 168 h

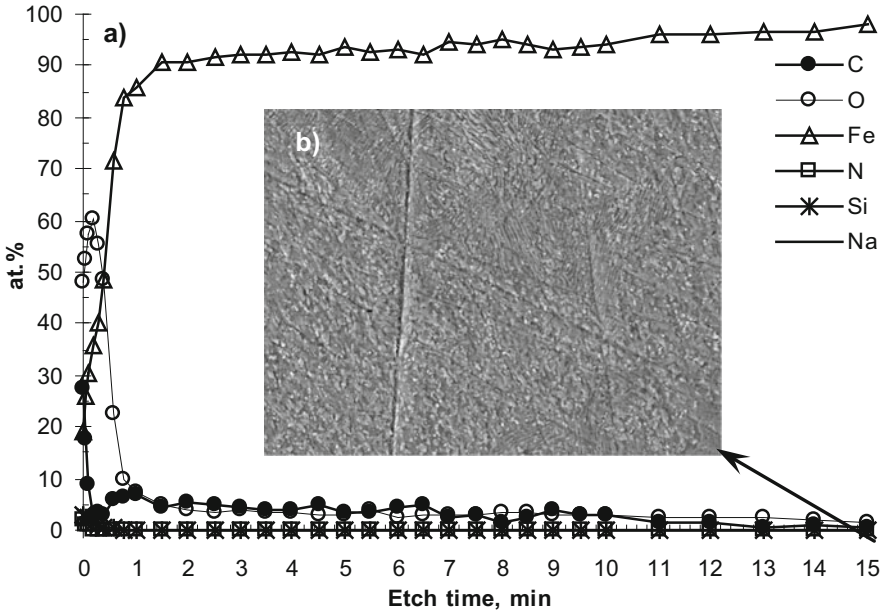

Fig. 5.14 Elemental composition of the protective film formed in the presence of synergistic mixture of $NaNO_2$ (10 mmol/l) + Na_2SiO_3 (20 mmol/l) at pH 10.2 obtained using Auger spectroscopy with ion etching against etching time (**a**) and sample morphology after ion etching (**b**)

nitrogen content and increased silicon content, similar to what is observed in the case of individual inhibitors (Fig. 5.14).

It should be noted that the surface morphology after ion etching shows characteristic signs of both additives. Mechanical treatment marks largely preserved as in the case of silicate, while some signs of metal dissolution process may also be observed as with sole nitrite. Taking into account the ability of $NaNO_2$ for a notable extent to promote the metal ionization process either individually or within a binary mixture, it is possible to use it for engineering optimal phase layer deposition conditions for complexing type inhibitors.

The isomolar series method has been employed for determining the optimal concentration ratio of the $NaNO_2$-PHMG binary mixture. It was found that the protective efficiency of the mixture against the concentration ratio has extreme character reaching a peak value of 99.8% at the $NaNO_2$/PHMG ratio as 2:1.

The SEM image of the surface layer after 168 h exposition revealed slight morphology changes compared to initial condition with marked smoothing of the mechanical treatment traces (Fig. 5.15).

The elemental composition of the protective film formed in the presence of synergistic mixtures of $NaNO_2$ + PHMG at optimal concentration ratio shows that the nitrogen content increased slightly from 20.6 to 25.5 at.% compared to sole PHMG that adequately corresponds to the presence of NO_2^- ions (Table 5.1).

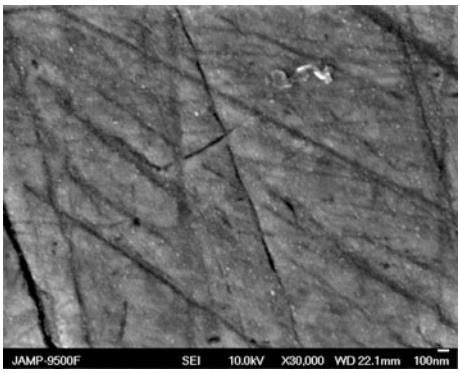

Fig. 5.15 Morphology of the surface after 168 h exposition in the presence of the $NaNO_2$ (20 mmol/l) + PHMG (10 mmol/l)

Table 5.1 Elemental composition of the carbon steel surface (by the results of Auger spectroscopy) after treatment in 1–30 mmol/l PHMG, 2–10 mmol/l PHMG, and 20 mmol/l $NaNO_2$

Spectrum	C	N	O	Na	Si	S	Cl	Fe	Total
1	49.3	20.6	17.7	–	–	0.1	–	12.2	100.00
2	48.1	25.5	22.3	0.5	1.8	0.1	0.1	10.9	100.00

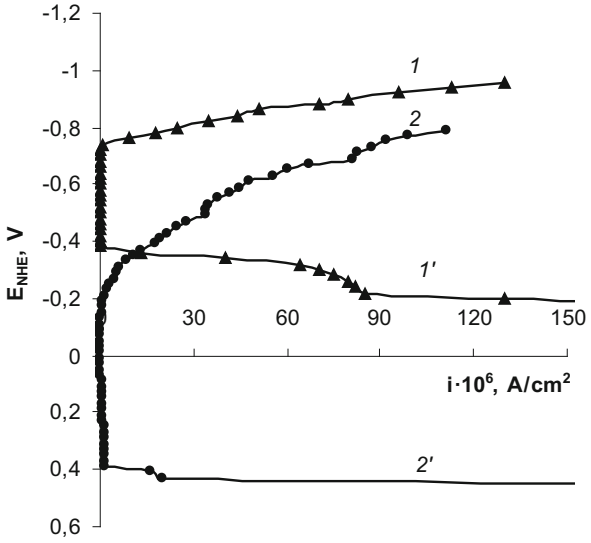

Fig. 5.16 Cathodic (*1, 2*) and anodic (*1′*, *2′*) polarization curves for carbon steel: *1, 1′*, background aqueous saline solution; *2*, *2′*, in the presence of $NaNO_2$ (10 mmol/l) + Na_2SiO_3 (20 mmol/l) at pH 10.2

Due to the formation of dense composite passive layers on the metal surface, the synergistic compositions of the inhibitors cause significant shift of the corrosion potential to the positive direction and form a long passivation zone in a wide range of potentials (1 V), and the potential of pitting formation is considerably distant from the corrosion that allowed to achieve full reliable protection of metals (Fig. 5.16).

In contrast, the efficiency of PHMG + Na_2SiO_3 mixture is unstable in the case of slight shift from the optimal concentration ratio of 1:1. This effect may be attributed

to mechanism concurrency as both mixture components require the metal cations to be able to form a phase layer.

Thus, the analysis of possible concurrent and complement effects between individual mechanisms and specific action of the mixture components is a crucial requirement for developing the efficient metal surface modification methods based on the formation of phase protective layers in multicomponent systems.

5.4 Conclusions

The processes of formation of phase protective layers in the presence of numerous individual inhibitors and their mixtures have been investigated. Thermodynamic approach for the analysis of possible interactions and equlibria based on the Pourbaix diagram has been demonstrated. It was shown that the pH value of the medium may significantly affect the protective efficiency and mechanism of action of the additives, as well as morphology of the formed phase layers.

Auger spectroscopy with ion etching enabled to confirm the mechanism of action of the additives and determine the thickness of phase layers and the composition distribution within protective films. Depending on the additives used for the formation process, the phase layer thickness varies in range from 15 to 50 nm.

Based on the obtained results, the generalized design recommendations may be proposed. The most efficient inhibitive mixtures may be composed using additives with different mechanisms of action that exhibit synergistic effects. In contrast, it was shown that additives with similar protective mechanism may demonstrate unreliable results due to mechanism concurrency.

Thus, the challenge of elaboration of modern surface engineering methods may be addressed by improving veracity of the theoretical models that represent the interaction in target systems in conjunction with recent advancements in the field of nanoscale systems.

References

1. Rozenfeld IL (1977) Corrosion Inhibitors. Khimiya, Moscow
2. Antropov LI, Makushin EM, Panasenko VF (1981) Inhibitors of the corrosion of metals. Tekhnika, Kiev
3. Tzaneva B (2013) Effect of pH on the corrosion behaviour of high nitrogen stainless steel in chloride medium. J Chem Technol Metall 48(4):383–390
4. Cui J, Yuan W, Yuan D, Pei Y (2017) Effect of pH on the passivation of carbon steel by sodium borosilicate controlled-release inhibitor in simulated recirculating cooling water. Ind Eng Chem Res 56(25):7239–7252. https://doi.org/10.1021/acs.iecr.7b01433
5. Hussain RR (2014) Passive layer development and corrosion of steel in concrete at the nanoscale. J Civil Environ Eng 4:e116. https://doi.org/10.4172/2165-784X.1000e116
6. Ledovskykh VM, Vyshnevska YP, Brazhnyk IV, Levchenko SV (2017) Metal surface modification for obtaining nano- and sub-nanostructured protective layers. Nanoscale Res Lett 12:186–191. https://doi.org/10.1186/s11671-017-1964-5

7. Ledovs'kykh VM, Vyshnevs'ka YP, Brazhnyk IV, Levchenko SV (2017) Development and optimization of synergistic compositions for the corrosion protection of steel in neutral and acid media. Mater Sci 52(5):634–642. https://doi.org/10.1007/s11003-017-0002-1
8. Ledovskikh VM (1983) Synergetic inhibition of steel corrosion in neutral media by nitrogenous organic alkalis with sodium nitrite. Prot Met 19(1):84–91
9. Min J, Park JH, Sohn H-K, Park JM (2012) Synergistic effect of potassium metal siliconate on silicate conversion coating for corrosion protection of galvanized steel. J Ind Eng Chem 18(2):655–660. https://doi.org/10.1016/j.jiec.2011.11.057
10. Truc AT, Pébère N, Xuan Hang T, Hervaud Y, Boutevin B (2002) Study of the synergistic effect observed for the corrosion protection of a carbon steel by an association of phosphates. Corros Sci 44:2055–2071. https://doi.org/10.1016/S0010-938X(02)00013-6
11. Pourbaix M (1974) Atlas of electrochemical equilibria in aqueous solutions. National Association of Corrosion Engineers, Houston, p 551
12. Ledovs'kykh VM, Levchenko SV, Tulainov SM (2013) Synergistic extrema of the mixtures of corrosion inhibitors for metals in aqueous salt solutions. Mater Sci 49(6):827–832. https://doi.org/10.1007/s11003-014-9680-0